Ice Distribution in Arcadia Planitia, Mars

Ali M. Bramson and Alexander Prescott

1. Introduction

Many lines of evidence point to the existence of relatively pure, excess ice (higher water ice abundances than can fit into the pore spaces of the regolith) in the northern mid-latitudes of Mars. Geomorphological evidence includes thermokarstically expanded craters [Viola et al. 2015], scalloped depressions [Dundas et al. 2015] and ice-exposing impacts [Dundas et al. 2014]. Additionally, Shallow Radar (SHARAD) sounding of the subsurface detects dielectric interfaces at these latitudes that have been attributed to the bottom of excess ice layers in the subsurface [Bramson et al. 2015]. Within the region of Arcadia Planitia, Mars, all of these types of features have been detected. We began this project with the assumption that all the excess ice features will correlate well spatially with each other. The motivation behind this project was to investigate the ice distribution using machine learning to help us determine where ice is, and where it is not. Bramson et al. 2015 suggested the ice sheet extended across the entire region, even though the radar detections did not; their thinking being that the ice sheet just became too thin to be detectable in regions without a detection due to the presence of terraced craters across regions even without radar detections. The initial research questions we wished to test with this project was:

a. What distribution of excess ice in Arcadia Planitia is predicted by Machine Learning based on the numerous lines of evidence for ice?
b. What does this distribution say about the probability that ice exists in each 1° by 1° latitude and longitude bin in the region, and the relationships between different geomorphic features across Arcadia Planitia?

2. Data

Multiple data sets spanning Arcadia Planitia were used in this project, provided by researchers at the University of Arizona Lunar and Planetary Lab and U.S. Geological Survey (USGS). Maps of terraced craters and SHARAD subsurface radar reflections were provided by Ali Bramson. Expanded secondary clusters, expanded craters on double layered ejecta craters, and expanded secondary crater clusters were provided by Donna Viola. Thermokarstic terrain and new impact craters that exposed ice (or not) were provided by Colin Dundas (USGS).

The terraced craters (TC) dataset includes positively identified TCs in the Arcadia Planitia region. The terraces in the walls of these craters indicate that the impact penetrated through different layers, suggested to be ice by the analysis of Bramson et al. 2015. The Shallow Radar (RADAR) dataset includes measurements where a subsurface reflector was positively identified that Bramson et al. 2015, interpreted to be coming from the bottom of an ice layer. Expanded craters exhibit thermokarstically-expanded crater boundaries due to the sublimation of ice after the initial impact. Expanded craters exist in clusters of secondary craters (CLUSTERS_exp), on double-layer ejecta (DLE_exp), and in secondary craters individually mapped (SEC_exp). Thermokarst (KARST) features occur when subsurface ice sublimates, leading to the collapse of

the overlying regolith, resulting in ‘scalloped’ landforms. New impacts (NEW) come from an analysis of HiRISE images, wherein re-imaging of a location reveals a new impact crater since the initial image. These craters can contain visible ice -- only those with visible ice are used in this project.

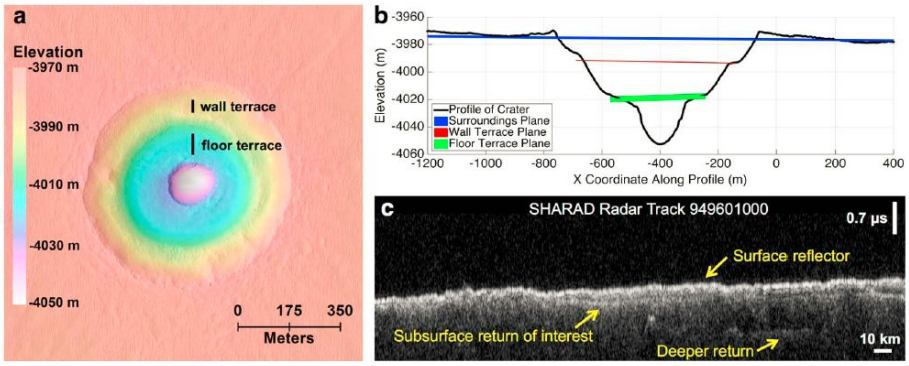

Figure: From Bramson et al. 2015 a) plan view and b) profile of an example terraced crater, and c) an example SHARAD transect with shallow subsurface reflector;

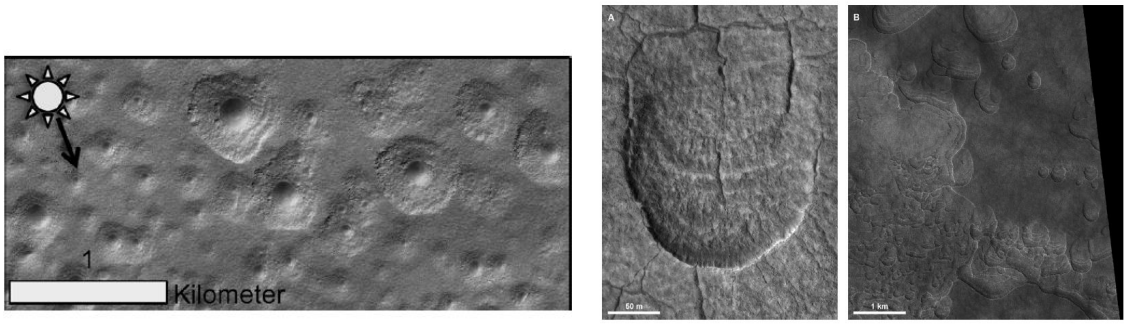

Figure: (left) from Viola et al. 2015: example of expanded craters; (right) from Dundas et al. 2015, example of scalloped terrain

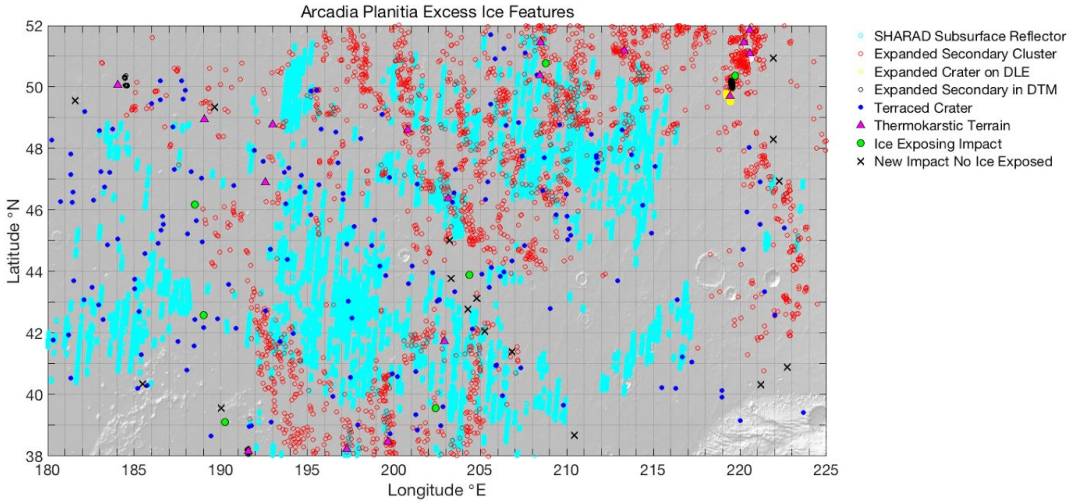

Figure: compilation of the input datasets across Arcadia Planitia.

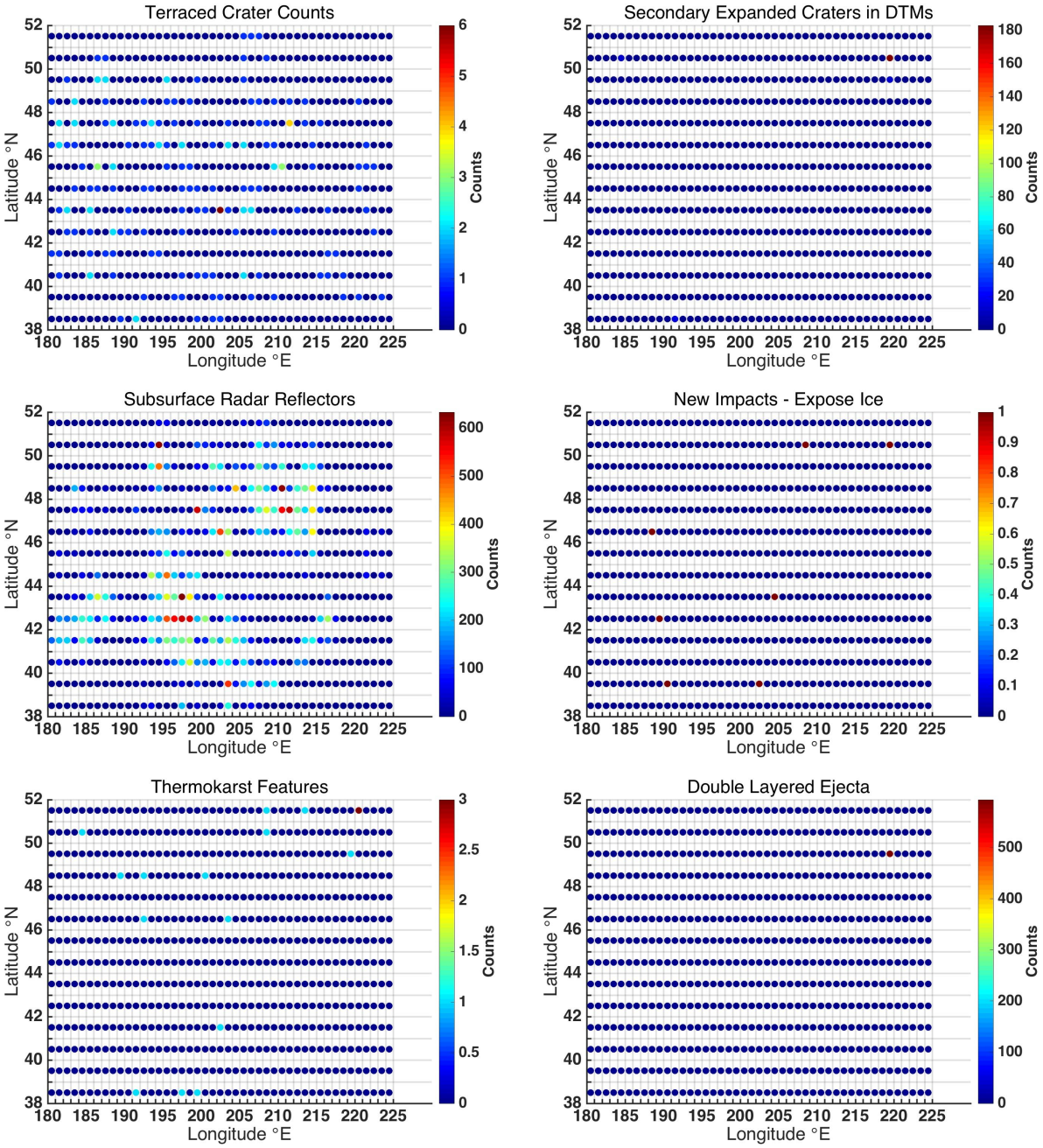
Terraced Crater Counts
Secondary Expanded Craters in DTMs
Subsurface Radar Reflectors
New Impacts - Expose Ice
Thermokarst Features
Double Layered Ejecta
Latitude °N
Longitude °E
Counts

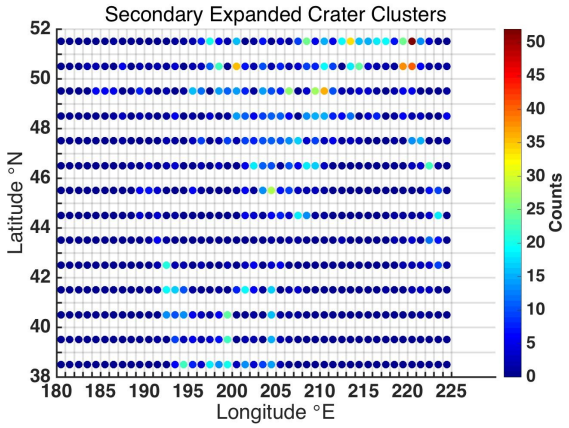

Figure: Maps of the count of each feature type across Arcadia Planitia.

3. Methods

The datasets were trimmed to include only data from 38°-52°N, and 180-225°E. Our model was then binned to a resolution of 1° latitude by 1° longitude, resulting in 630 pixels. The latitude and longitude for every instance of each feature type was used to count the number of instances of each feature in every pixel (i.e. number of subsurface radar detections within each pixel, or number of terraced craters in each pixel, etc.). This count matrix was used in our analysis (X0), as well as a matrix of the fractional distribution of each feature in each pixel (i.e. the count of instances in a given pixel divided by the total number of instances of that type of feature).

We use 7 different permutations and manipulations of the features as inputs to k-means clustering and t-SNE dimensionality reduction to visualize and explore this dataset.

- **X0**: pure counts of each feature, unnormalized
- **X1**: fractional values (each feature is normalized to the total number of counts of that type of feature), with SEC_exp and DLE_exp scaled to have the same mean fractional value as RADAR. These 2 features are highly localized and thus have relatively very large fractions. The scaling is meant to decrease their misleading inflated fractional importance and make them of equal importance as an average non-0 RADAR pixel
- **X2**: fractions with SEC_exp and DLE_exp features removed
- **X3**: in every pixel, each feature is represented in binary as present (1) or not (0)
- **X4**: fractions with only TC, RADAR, and CLUSTERS_exp included. These three datasets are the most spatially complete
- **X5**: the same as X4, but all normalized to have the same mean fractional value as radar
- **X6**: X2 (local datasets removed) turned into binary pixels for each feature as either present, or not (like X3) and then summed into one feature between 0 (no features of any sort in that pixel) and 5 (every type of feature present in that pixel).

4. Results

4a. X0

While this input gives the best silhouette plot (most coefficients in the clusters near 1), this is likely forced by the huge number of radar data points relative to everything else. This is apparent in the plotting of features colored by cluster - only radar clustering shows structure correlated to cluster assignment. The t-SNE plots also show very little in terms of structure/logical clusterings. Two t-SNE plots are shown to demonstrate the importance of the perplexity parameter, at least in this poorly cluster-structured data. We found we had to ramp the perplexity way up (greater than the number of pixels divided by 2 - over an order of magnitude higher than the default value of 30) to develop some sort of structure.

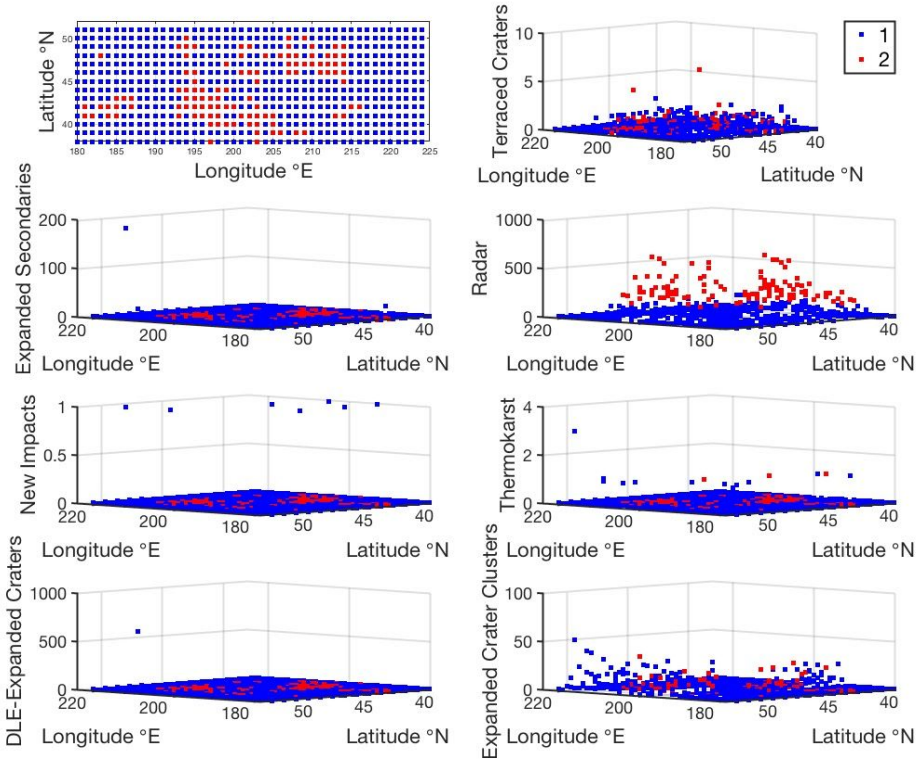

Figure: Plots of the k-means cluster classifications for 2 clusters on input X0 shown in 2D on a map of latitude and longitude (top left) and in 3D versus each of the input features contained in X0. Only the radar counts show correlation between value and cluster classification (where a cluster of 2 is the presence of a subsurface radar detection and cluster 1 is no radar detection).

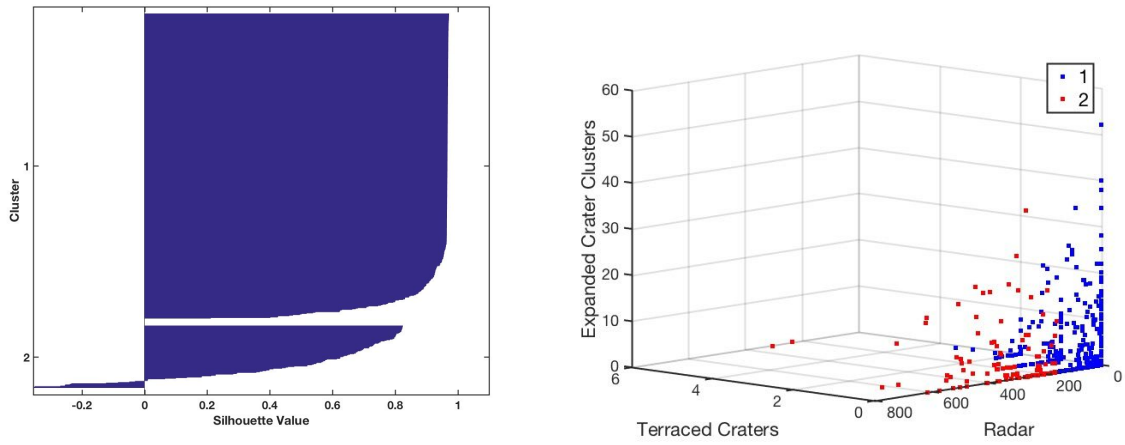

Figure: (left) k-means silhouette plot showing most coefficients are close to 1, suggesting reasonable confidence that each point is assigned to the right cluster. However, this was because the values in the radar counts are so much higher than all other datasets, it basically only classified the data by if it had a radar signal or not. (right) Plot showing the relationship in multidimensional space of the three most complete datasets (terraced craters, radar and expanded crater clusters) and the clusters outputted by k-means.

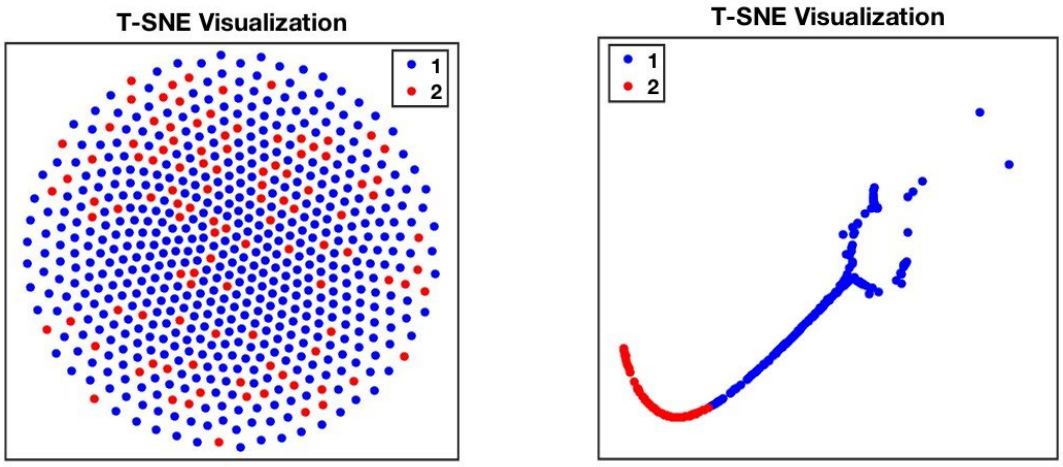

Figure: (left) t-SNE results for perplexity of 300 or lower, showing no structure, (right) t-SNE results for perplexity of 500, yielding structure, though no strong link to k-means clustering results (red and blue)

4b. X1 and X2

Both of these inputs were found to yield very bad results, making two very unevenly sized groups, merely deciding to make the clusters based on the small dataset of new impacts. For both of these results, the silhouette plot shows that most points classified as a 1 have a negative silhouette coefficient, suggesting the algorithm has little confidence that points in this grouping were classified correctly. The results also changed between different runs of these inputs; in one run, k-means would make its clusters purely by the small new impact feature,

other times by the presence of thermokarst (also a relatively small set of data within the different features used). When X1 and X2 were run through k-means with 3 clusters, the algorithm decided to make three clusters based simply on the presence (or not) of these features (cluster 1 generally has neither feature; cluster 2 has thermokarst features; cluster 3 has new impacts). The results of the various k-means experiments performed on X1 and X2 demonstrate that the algorithm was fairly arbitrarily deciding to use features with binary values to determine clustering, rather than finding an illuminating way to cluster the data based on a combination of features.

X1 (run 1)

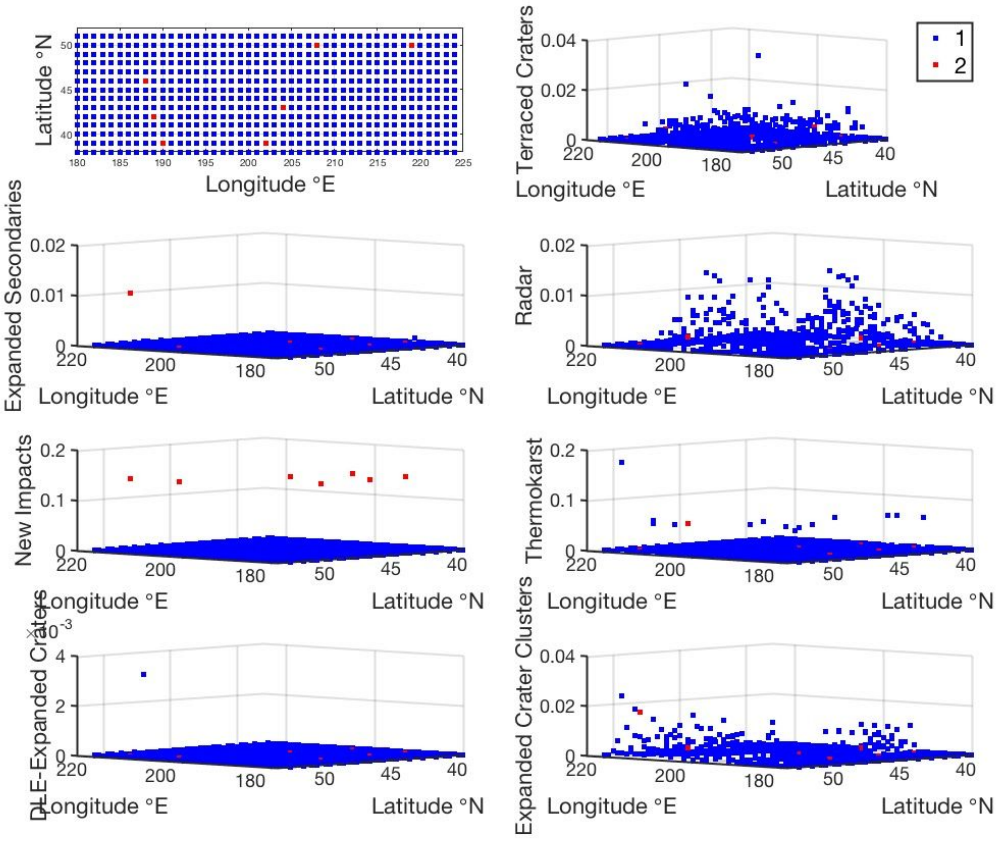

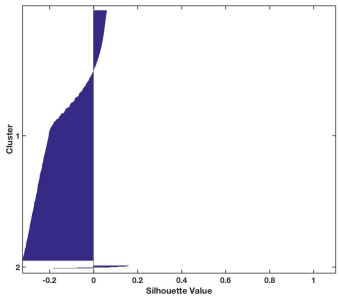

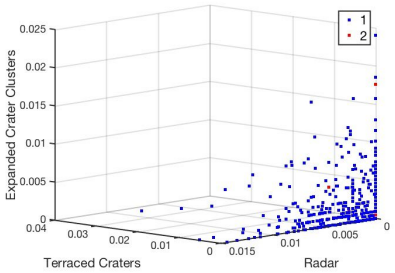

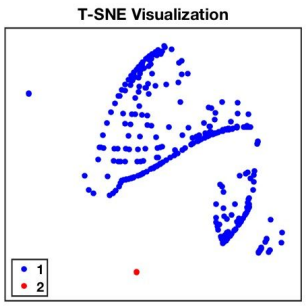

X2 (run1)

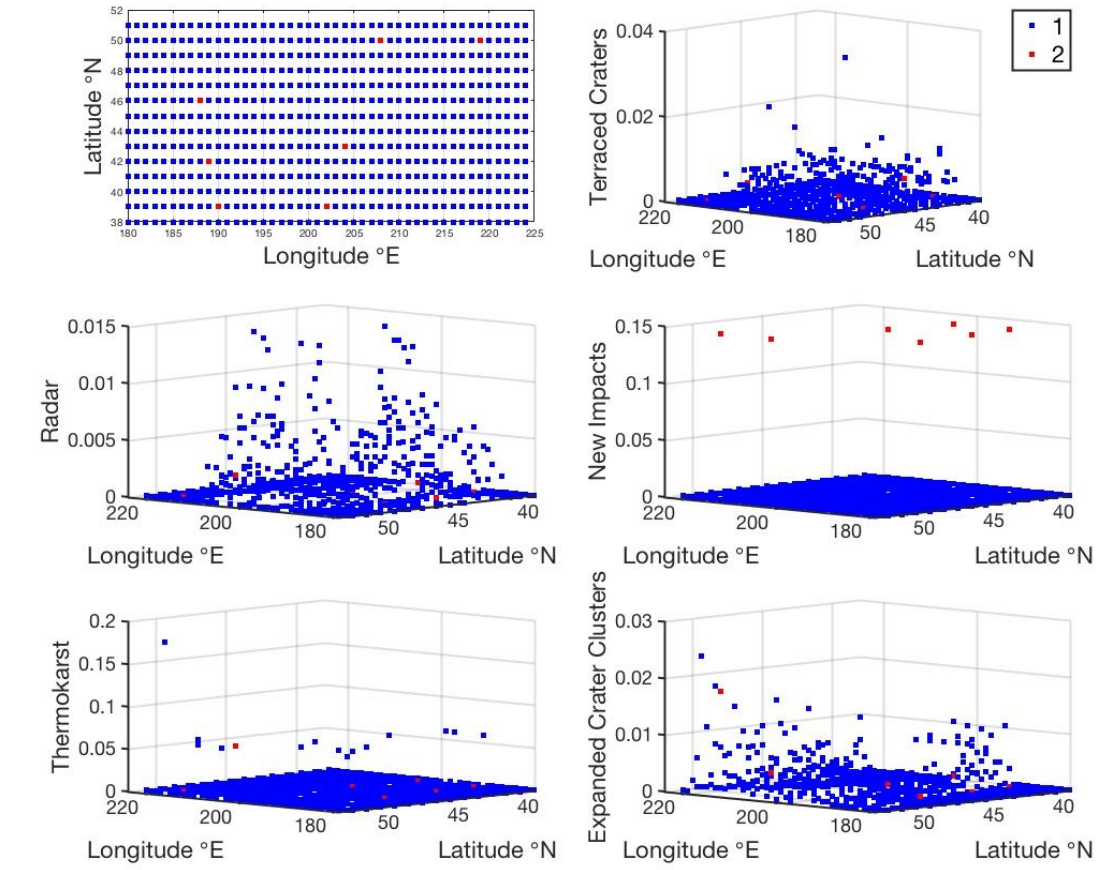

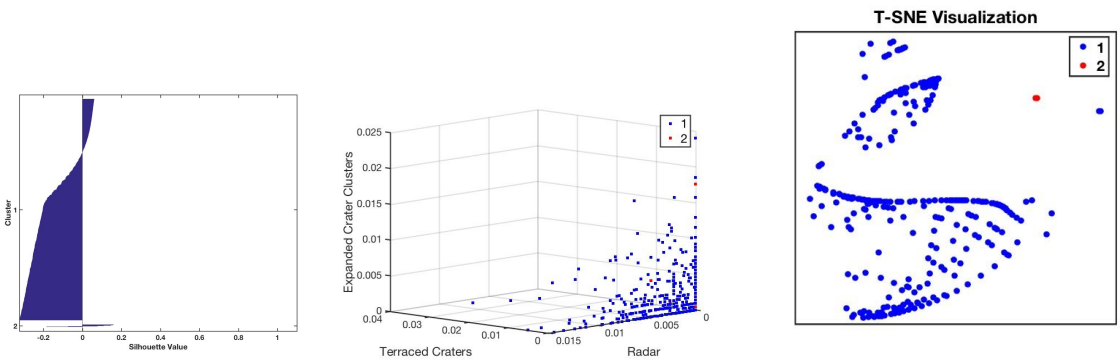

4c. X3

X3: Looking at the plots of feature type colored by cluster, the k-means algorithm clearly chose to cluster the data based on the expanded crater clusters feature alone. The silhouette plot indicates some good clustering, but still much of the data may be incorrectly clustered. The

t-SNE results show the best separation between clusters, but the points are not well clustered within themselves.

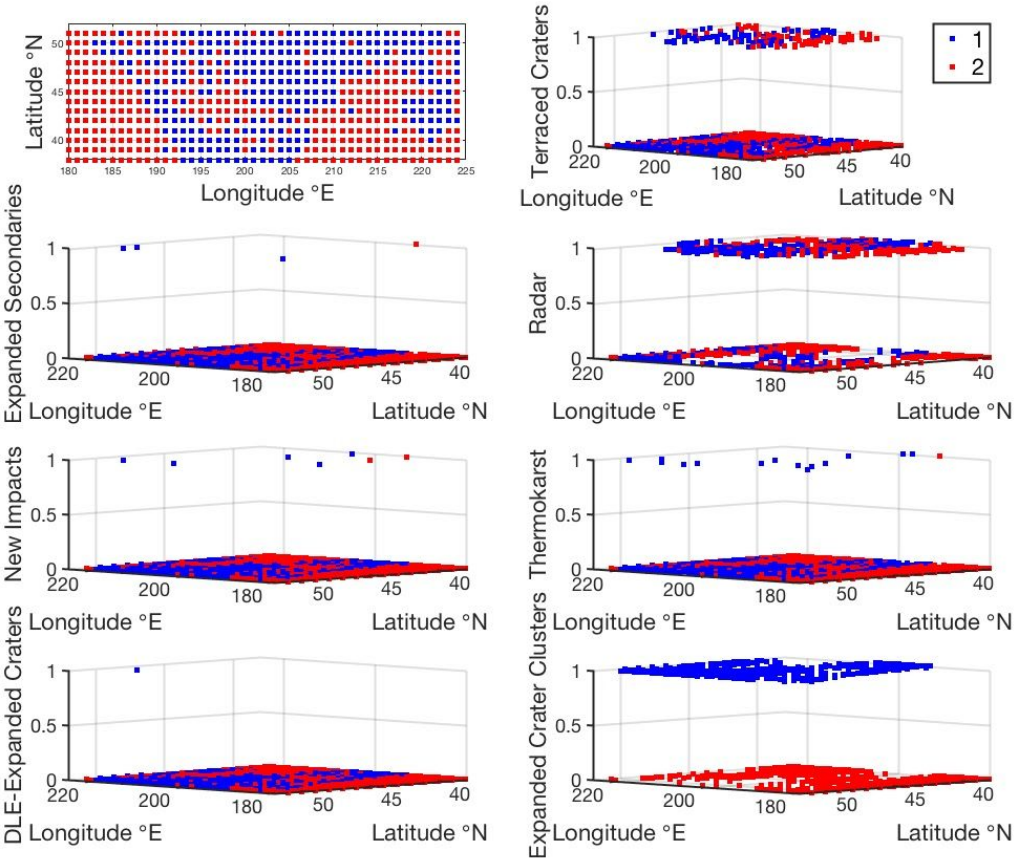

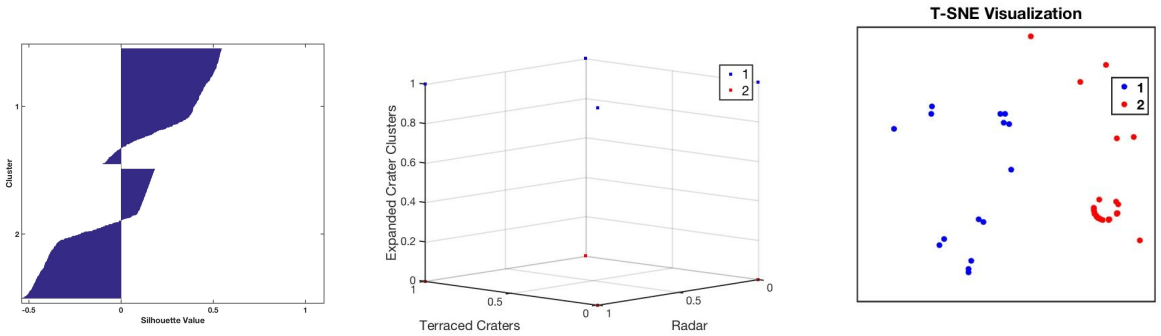

4d. X4

In runs using this input, we find decent separation of clusters in the t-SNE plot, with some intracluster grouping as well. The feature plots show that k-means separated the data based on terraced craters alone, with radar and expanded crater clusters randomly clustered. This indicates that these three datasets, which are the most regionally distributed, are not well correlated with each other. Other runs show that k-means will form its clusters based on

expanded crater clusters as well, but that leads to the terraced crater cluster plot becoming random. Different runs yielded different clustering based on different thresholds, meaning some outputs only had 4 pixels in cluster 2 (the 4 pixels where there are several terraced craters), and all other pixels being clustered together. This, and the silhouette plot, demonstrates that the algorithm is not confident in clustering based on any one feature alone, yet it cannot properly find any clusters successfully using both features. When k-means was performed with 3 clusters, the algorithm classified the data into which pixels had terraced craters, which had many expanded crater clusters, and which had neither; the radar values in this output were randomly distributed. This again shows that we cannot find a correlation simultaneously between radar detections, terraced craters and expanded crater clusters.

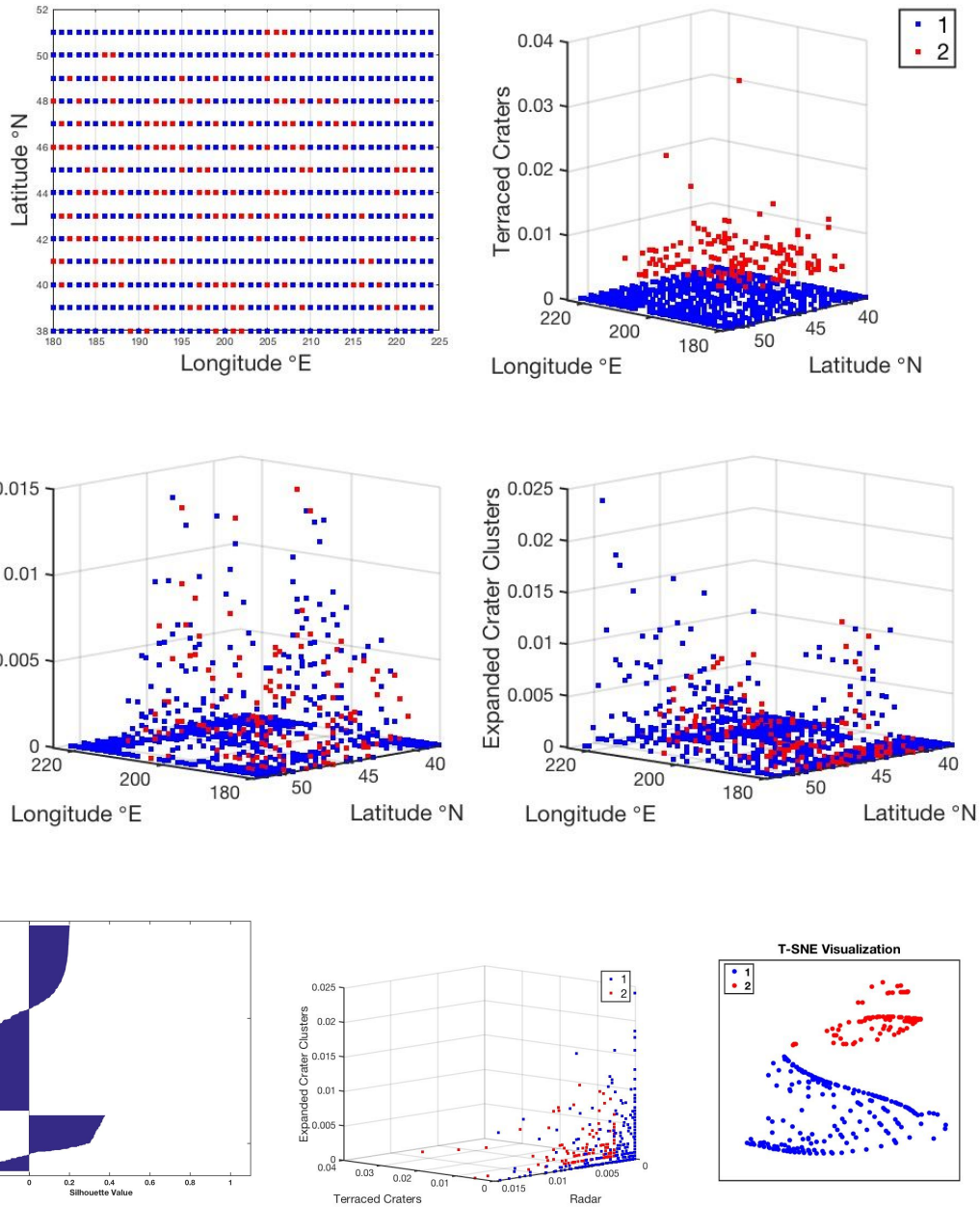

4e. X5:

The t-SNE results are very bad and the silhouette results are not great, although somewhat interesting. Clusters 1 and 3 (i.e the 'yes ice' clusters) show that about half of each cluster was probably clustered correctly but that the other half may not have been clustered correctly. Meanwhile in cluster 2, the 'no ice' cluster, all of the points may have been incorrectly clustered. This illustrates our lack of knowledge of whether or not excess ice actually exists in those areas and thus a lack of understanding in the regional extent of that ice. It is entirely possible that the entire region, at 1° by 1° resolution, is underlain by excess ice. The feature plots indicate that

k-means clustered the data based on radar (cluster 3) and expanded crater clusters (cluster 1). Interestingly, increasing the number of clusters to 4 did not serve to create another cluster that corresponded to terraced craters - the clusters showed no additional structure. The randomness shown in the terraced crater clustering further indicates the independence of each of these datasets, and could suggest even an anti-correlation in radar and expanded crater clusters given it separated these features into different clusters.

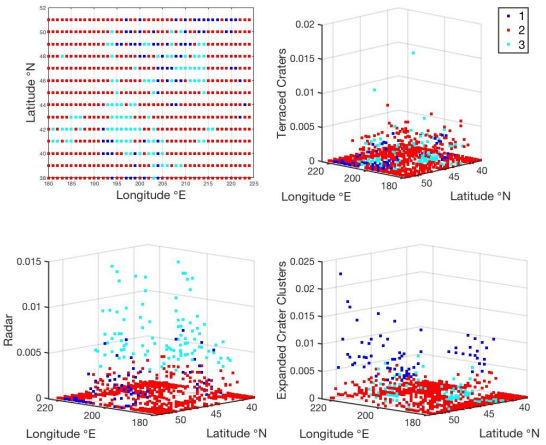

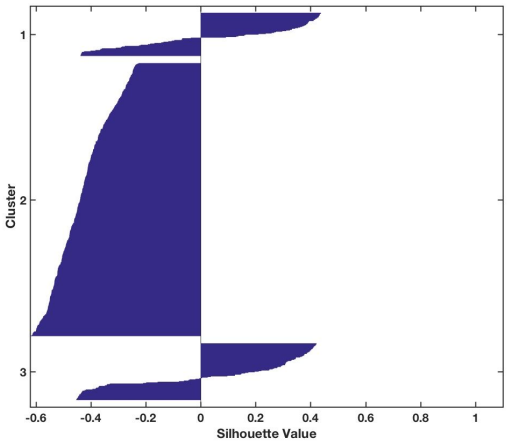

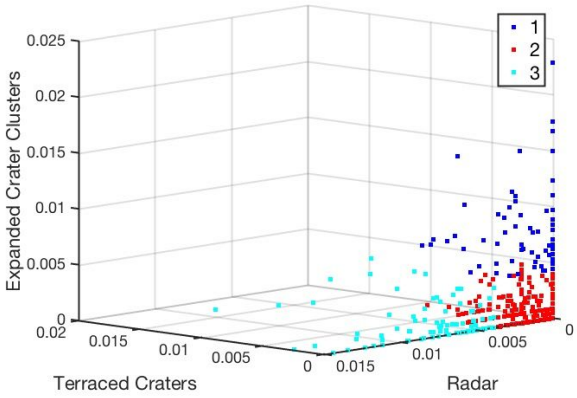

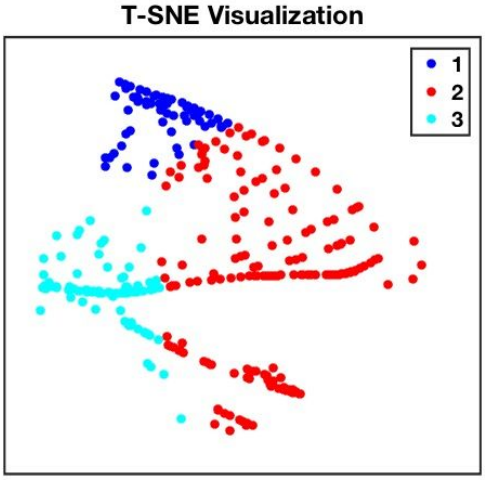

4f. X6

The k-means results for 2 clusters (left) and 3 clusters (right) are shown here to illustrate that simply using the sum of whether or not a feature exists in a pixel only results in clusters reflecting exactly what one would expect. For 2 clusters, all of the pixels with at least one feature are grouped together, while for 3 clusters an additional group is created for counts greater than 3.

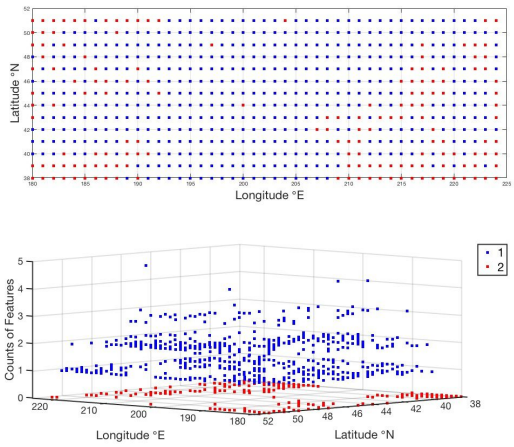

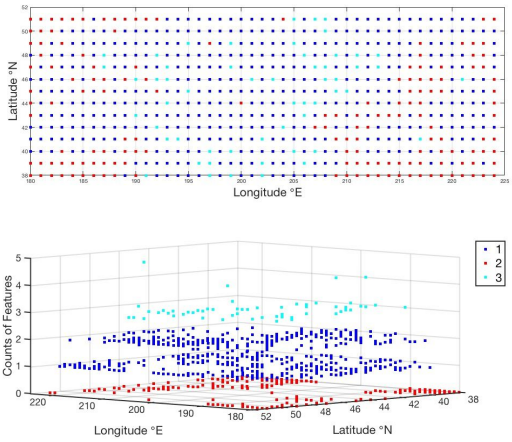

5. Conclusions
    a. Different results for the same inputs to k-means indicate multiple solutions for each input dataset permutation.
    b. Many of the features are often used as the sole classifier of cluster, with the results for the other features showing random clustering. This suggests many of the features are not correlated to each other. Additionally, the spatial distribution of subsurface radar detections vs. expanded craters may even show an anti-correlation. This opens up additional future questions as to why this lack of correlation exists in these regional datasets, and why expanded craters are not linked to the presence of subsurface radar detections (both inferred to be formed from the same excess ice sheet). Is there a geologic interpretation for the lack of correlation between features (and inverse correlation between the two most widespread datasets), or is this distribution by chance?
    c. We find negative values across silhouette plots for all k-means runs performed for this project (other than the run that just uses radar and basically ignores all other features), suggesting a lack of confidence in classifying pixels into clusters based on the features we have.
    d. This project reflects the importance of having a known map of ice coverage, or some other related ‘known’ quality, to train a machine learning algorithm. This is true for supervised learning as well as unsupervised learning, as it is not possible to rigorously inspect the validity of an unsupervised learning algorithm without some sense of the actual distribution of ice. This is especially true because of the lack of correlation between features and confidence in the the algorithm’s clusters.
    e. Machine Learning did not help in this project to answer the initial research questions, i.e. what is the distribution of excess ice in Arcadia Planitia? And what is the probability that ice exists in each 1° by 1° pixel in the region? It did help us learn that there does not appear to be an easily-classifiable connection between all of the ice-related data that exist across Arcadia Planitia.

f. Qualitatively, inspection by eye of the map of excess ice features across the region does as-good of a job or better at getting a sense of where excess ice is located, and the relationship between ice-related features, than this implementation of k-means.

6. References

Bramson, A. M., S. Byrne, N. E. Putzig, S. Sutton, J. J. Plaut, T. C. Brothers, and J. W. Holt (2015), Widespread excess ice in Arcadia Planitia, Mars, Geophys. Res. Lett., 42, 6566–6574, doi:10.1002/ 2015GL064844.

Dundas, C. M., S. Byrne, A. S. McEwen, M. T. Mellon, M. R. Kennedy, I. J. Daubar, and L. Saper (2014), HiRISE observations of new impact craters exposing Martian ground ice, J. Geophys. Res. Planets, 119, 109–127, doi:10.1002/2013JE004482.

Dundas, C. M., S. Byrne, and A. S. McEwen (2015), Modeling the development of martian sublimation thermokarst landforms, Icarus, 262, 154-169,doi:10.1016/j.icarus.2015.07.033

Viola, D., A. S. McEwen, C. M. Dundas, and S. Byrne (2015), Expanded secondary craters in the Arcadia Planitia region, Mars: Evidence for tens of Myr-old shallow subsurface ice, Icarus, 248, 190-204, doi:10.1016/j.icarus.2014.10.032